ADDITIVE MANUFACTURING OF FUNCTIONALLY GRADED MATERIALS WITH IN-SITU RESOURCES

I. Cheibas[(1)], M. Laot[(2)], V.A. Popovich[(3)], B. Rich[(4)], S. Rodriguez Castillo[(5)]

[(1)(4)(5)]ESA/ESTEC European Space Agency, Keplerlaan 1, 2201 AZ, Noordwijk, The Netherlands, Email: ina.cheibas@gmail.com, belinda.rich@esa.int, sarah.rodriguez.castillo@esa.int
[(2)(3)]Delft University of Technology, Department of Materials Science and Engineering, 2628 CN Delft, The Netherlands, Email: M.A.L.Laot@student.tudelft.nl, V.Popovich@tudelft.nl

KEYWORDS

Functionally Graded Materials
Additive Manufacturing
Digital Light Processing
Spark Plasma Sintering
In Situ Resource Utilization
Regolith

ABSTRACT

This study examines the additive manufacturing feasibility of functionally graded materials with in-situ resources. A potential application of the outcome is for aerospace components and space habitats. At first, compatible in-situ resources for functionally graded materials and additive manufacturing (AM) suitable processes are investigated. Then powder characterization of three lunar simulants is performed to evaluate them for the fabrication tests. The chemical compositions, particle shape and size distribution, and thermal characteristics of the powders were analysed.
This paper is a part of an ongoing study, with a final aim to develop a functionally-graded composite at the level of concept validation and evaluate it for thermal and mechanical properties.

1. INTRODUCTION

Successful long-term space exploration missions must ensure a high level of security and safety against harsh environmental conditions, such as meteoroids, radiation, thermal cycles, abrasion, vacuum, etc. Space habitats are a prospect in these missions. The building materials must ensure indoor atmospheric and thermal control whilst protecting from the outer space environment [1]. Space habitat designers and researchers generally propose resilient structures with multi-layered solutions, e.g., Fig. 1 [2][3]. Multi-layering is reasoned by a multitude of factors: mission requirements (both of the habitat itself and the need for configuration variety), user demands, and destination.

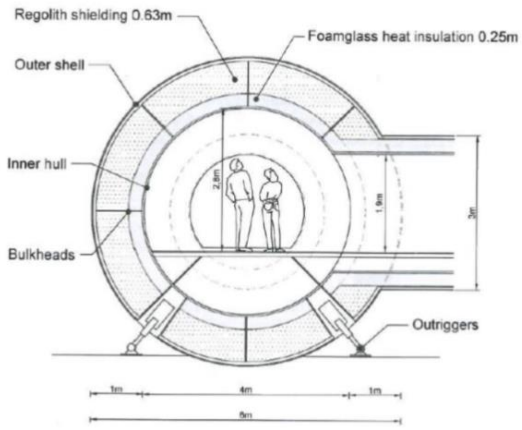

Figure 1. Section of a cylindrical module [4]

To overcome these requirements, NASA has proposed a strategy for technological habitation to be accomplished in three phases [5]:

- Class I, pre-integrated hard shell module;
- Class II, habitats prefabricated and surface assembled;
- Class III, in-situ resource utilization (ISRU), derived structure with integrated Earth components.

The designs for Class II and III modules usually consist of an interior shell pressurized containment and an exterior regolith layer to protect from radiation, meteoroids, and thermal cycles [6][7][8]. The proposals for the interior shell are generally

Earth-constructed, Fig.2 [4]. Shells can be built from textiles (inflatables), alloys, composites, etc. The exterior cover is recommended to be in-situ additive manufactured with regolith, due to the abundance of the loose material on planetary surfaces [9][10].

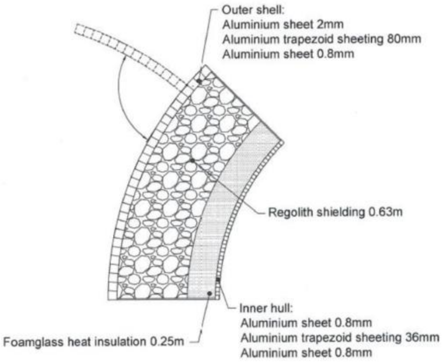

Figure 2. Double-shell structure wall section [11]

The reason for using regolith as a construction material is that it enables the use of resources available on-site, and diminishes significantly the payload's weight brought from Earth. It is therefore a key strategy in fulfilling the goal of sustainable and affordable human and robotic exploration [12].

1.1. Functionally graded materials

In a sustainable mission, the strategy for a Class III space habitat requires full integration of subsystems and fabrication with in-situ resources. However, current solutions make use of single-material manufacturing methods and regard regolith as an aggregate instead of a source for alloy extraction [2]. Even if resources are readily available for a Class III module multi-material fabrication, the construction methods are considered separate both for the interior and the exterior of the structure. Besides not exploring the full in-situ resource utilization (ISRU) potential, these fabrication methods might contribute to challenges regarding mismatch at the interface between materials, in terms of fretting wear, fatigue, fracture, corrosion, and stress corrosion cracking [13][14]. Functionally graded layers can serve as an optimal transition between two incompatible materials. They are designed with function or performance in a graduated morphology to achieve tailored features [15][16][17]. For example, a buffer layer at a ceramic-metallic interface improves compatibility by promoting stronger bonding between substrates and preventing delamination otherwise common in composites. Besides the benefit of improved mechanical behaviour, thermal properties can also be enhanced by a specific sequence of graded insulation layers [13][18]. Functionally graded materials (FGM) are considered advantageous in maximizing the capabilities of in-space resources due to their multi-material approach evaluated as high performance contrary to monolithic applications [19].

FGMs can be classified by four major distinct categories, namely: 1) volume fraction, 2) grain shape/size, 3) material fraction, and 4) orientation, Fig. 3. [21][22][24].

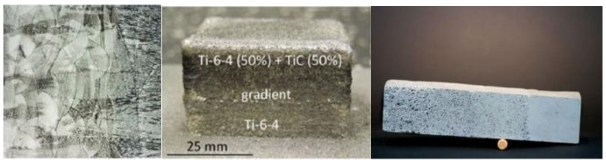

Figure 3. From left to right, a schematic diagram of gradient type: shape/orientation [25]*, material* [20]*, and volume fraction* [23].

Metal-ceramic gradients have been widely studied in recent years because of their attractive properties. There are a multitude of graded material examples that have shown high-temperature stability, high hardness, corrosion resistance, and good versatility; such as aluminium-silicon carbide (SiC/Al); aluminium-aluminium oxide (Al-Al_2O_3); titanium-titanium carbide (TiC/Ti) graded composites; graded yttria-stabilized zirconia coatings and Al_2O_3 ceramic coating on AZ91HP Mg alloy [14][26][27][28][29][30][31][32][33][34].

2. MATERIALS AND METHODS

This research is focused on the feasibility of ISRU via manufacturing of FGMs for a Class III space habitat. Because the study is considered for human space exploration, the Moon is selected as a strategic location in terms of planetary surfaces. The reasoning is based on Earth`s proximity to the Moon, as the closest and most reachable terrestrial body in case of emergency evacuation and supply. It is proposed that initial research for technology and human life support systems can be performed on a lunar habitat. Then the transfer of knowledge can be considered in future missions for other terrestrial bodies [2].

The primary resource for ISRU on the lunar surface is regolith, i.e. the layer of unconsolidated mineral of thickness between 3 - 20m atop the lunar surface, consisting of fine-grained particles and rocks [35]. The constituents of the lunar soil are comprised of silicate (plagioclase, feldspar, pyroxene, olivine) and oxide minerals (ilmenite, spinel) [36][37][35]. Other possible materials present in small quantities are volatiles (water, OH, H, C, N, F, S, Cl), however accurate soil composition will differ depending on the sampling location (Mare, Highlands) [38][39].

2.1. Metal extraction from regolith

To effectively locate, process, and utilize native resources is an essential mining requirement for lunar base operation. The lunar soil is abundant in metals such as silicon, aluminium, iron, titanium, and magnesium. Iron metal has potential structural purposes, while aluminium can be used as a coating metal, or rocket fuel [2]. The metal extraction methods from minerals are pyrometallurgy, electrometallurgy, and hydrometallurgy. In each discipline, the reduction of each component to its elemental form must have a process reactant that can be recycled indefinitely, be suited for lunar surface conditions, and consume minimal water [40]. Silicon, aluminium, and glass can be refined using fluorine, in a multi-stage reduction process that separates and purifies the elements. Oxygen is a by-product in this refining process, which is a high-priority resource for human life support or rocket fuel [38]. Molten salt electrolysis (Metalysis-FFC) technique has been tested on a lunar simulant JSA-2A to process metal alloys as products. The method produced three dominant distinct alloy groups, Al/Fe alloy, Fe/Si alloy (sometimes with the inclusion of Ti or Al), and Ca/Si/Al alloy (sometimes with the inclusion of Mg). Depending on the feedstock, Metalysis-FFC has the potential to produce specially-design alloys from refining of lunar regolith [41].

The extracted lunar resources considered for a gradient in the current study are titanium, titanium alloys, steel, magnesium, aluminium, and aluminium alloys. The primary criteria for material selection are simulant compatibility with the metal or alloy in particle size distribution, density, and thermal properties.

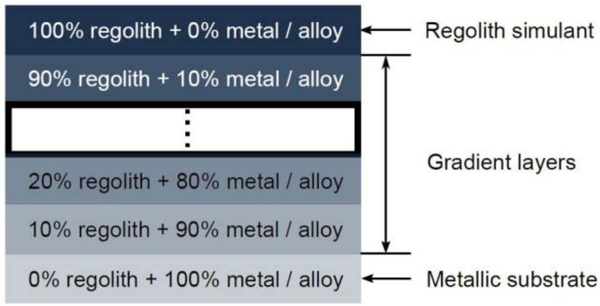

Figure 4. Framework for FGM materials.

Additive manufacturing (AM), also known as 3D-printing, can be used for FGM fabrication in a gradient from a) metal to a regolith simulant, or b) alloy to a regolith simulant, see Fig. 4. Similar to ceramic reinforced metal matrix composites (MMC), the chosen metallic substrate will be dispersed in the regolith matrix, a technique that may contribute strengthening to the additive manufactured regolith [42].

2.2. Additive manufacturing

Current FGM fabrication methods can be classified as thin-film or bulk fabrication. Thin sections/coatings have the advantage of being less time consuming, for which fabrication processes such as physical/chemical vapour deposition are generally applied [43]. Bulk FGMs are more demanding and commonly use conventional powder metallurgical technologies [44][24]. In this study, which focuses on the application of FGMs for components or a space habitat, bulk manufacturing techniques that could be considered include material extrusion [45][46][47], light polymerisation [48], spark plasma sintering [49], powder bed [50][51][52] and powder fed techniques [53][42][54].

The selection between AM and conventional methods depends upon technique viability for processing both ceramic and metal/alloy powders, suitability for microgravity, and resultant mechanical properties post-fabrication. Subsequently, the following methods are considered herein: (i) Spark Plasma Sintering (SPS) is selected due to the higher powder densification in the sintering technique, essential for building reliable structural components [49]; and (ii) Digital Light Processing (DLP) as this method works both with ceramic and metal powders whilst being suited to a microgravity environment [55].

An overview of the different promising consolidation techniques suitable for ISRU, as well as their advantages and disadvantages, is given in Table 1. It must be noted that none of the following studies have been conducted with genuine lunar regolith, rather with a variety of Earth-manufactured simulants. Thus results are expected to be partially dependent on the simulant properties and also on the chosen lunar environment for some early studies.

Table 1. Overview of advantages and disadvantages of consolidation techniques suitable for ISRU

Consolidation technique			Advantages	Disadvantages
Additive Manufacturing	Material Extrusion	**Sulfur Concrete** [56][46]	• Ease of manufacturing • Presence of FeS on the Moon • Cheap process	• Feasibility of extraction of S from ores • Low impact resistance • Relatively high rate of sublimation of S
	Power Bed Fusion	**Selective Laser Melting (SLM)** [57][58]	• Can produce high quality components in low to medium batch quantities • Good repeatability • Full design flexibility • Low waste compared to conventional casting techniques (no machining) • Production of nearly fully dense parts	• Slow process and poor surface finish • Residual stresses (cracking) • Porosity (requires post-processing) • Lack of knowledge about the interaction between laser and ceramics • Powder sieving or crushing required • Powder heterogeneity causes variations in energy density
		Solar Sintering [59][60]	• Use of solar light source, more stable on the Moon • No need of binders	• Difficulty when sintered under vacuum • Low mechanical properties • Poor bonding between successive layers • Difficult to balance sintered and molten phases • No prediction on the equipment lifetime • Few investigations carried out on this technique
	Binder Jetting	**D-shape Process** [61]	• Allows large-scale manufacturing in one single printing process • No need of sieving or crushing of the lunar regolith	• Large printer must be brought to the Moon • Use of an inorganic binder and an ink • Large quantity of binder • Low shape accuracy • Multistep process lasting several hours
	Photopoly-merization	**Stereo-lithography** [62][63]**/ Digital Light Processing (DPL)** [48][55]	• Good surface finish • More accurate and complex shape can be produced by this technique • Can produce small parts with high precision but also large parts whilst maintaining high precision • No mould required, only a CAD model	• Requires specific polymeric resins and additives • Time demanding (multistep process lasting several hours) • Expensive process • Difficult to achieve high density • Complex curing process and complex kinetics • Smaller (down to nano) particle size is preferred

Conventional fabrication	**Spark Plasma Sintering (SPS)** [64][49]	• Microstructure control due to low temperature and short time • High density due to higher heating rate and pressure than other techniques • Dissimilar materials can be sintered • Fast and FGMs can be produced • Cost of SPS is 50 – 80% lower than other conventional sintering techniques • Temperature of 900°C enough for sintering lunar regolith • Good mechanical properties	• Only simple symmetrical shapes can be prepared • Expensive DC generator required • For very small powders (less than 100 nm), significant temperature gradient can lead to non-uniform densification • Sieving or crushing required for lunar regolith • Limited to simple shapes
	Vacuum Sintering [65]	• Sintered parts with low thermal conductivity • Prevention of oxidization	• High weight loss increasing with temperature • Presence of macro-pores, which can be controlled with sintering temperature • Shrinkage dependent on the temperature
	Thermite reactions [66][67]	• Reduction of energy needed • Limited equipment is required • Quick reactions with smaller particles	• Addition of Al and other substances like Teflon • Porous structures • Little information about mechanical properties • Sieving or crushing required for lunar regolith • Deformation and surface cracking (even more with smaller particles)

3. PROCESS MATRIX CHARACTERIZATION

Due to the limited availability of original lunar soil, the current study is conducted with three regolith simulants: EAC-1A, LMS-1 (Lunar Mare Simulant), and LHS-1 (Lunar Highlands Simulant), (see Tab. 2 for composition). Selection of these simulants is based on resemblance to Apollo sample bulk chemistry, and mineralogical diversity of the location (Mare and Highlands) as also shown in Tab 2. LMS-1 and LHS-1 have been developed by CLASS Exolith Lab. The simulants were manufactured by combining both mineral and rock fragments (i.e. polymineralic grains) for high-fidelity attributes [68]. EAC-1A lunar simulant was developed by the European Astronaut Centre (EAC) in Cologne. The powder was sourced from a commercial quarry in the Eifel volcanic region in Germany [69].

The considered processes, Digital Light Processing (DLP) and Spark Plasma Sintering (SPS), require characterization of the lunar simulant to determine and predict the fabrication behaviour. Bulk chemistry, particle shape, and size distribution are essential properties and have been investigated in this study for all three simulants.

3.1. Bulk chemistry and mineralogy

Apollo missions and robotic lunar landers are the benchmark for the development of LHS-1 and LMS-1 simulants. The reference materials for LHS-1 and LMS-1 simulants are the Generic Highlands Soil and High-Ti Mare Soil respectively, see Tab. 2, and Tab. 3. Lunar Highlands soils are predominantly comprised of anorthosite, a rock which is largely made up of plagioclase feldspar. Lunar Mare soils contains volcanic rock that erupted at the lunar surface and produced lava flows and pyroclastic deposits [70].

Table 2. Oxide composition of lunar simulants EAC-1A [71], *LMS-1, LHS-1* [68], *JSA-2A* [71], *and lunar samples Apollo 17 High-Ti Mare (71055) and Apollo Highland Average chemical composition* [70].

	EAC-1A	**LMS-1**	**LHS-1**	**JSA-2A**	**Apollo 17**	**Apollo Highland**
Units	*(wt%)*	*(wt%)*	*(wt%)*	*(wt%)*	*(wt%)*	*(wt%)*
SiO_2	43.70	42.18	44.18	47.50	37.60	45.50
TiO_2	2.40	4.62	0.79	1.50	12.10	0.60
Al_2O_3	12.60	14.13	26.24	15.00	8.74	24.00
Cr_2O_3	-	0.21	0.02	-	0.42	-
Fe_2O_3	12.00	-	-	3.50	21.50	5.90
FeO_T	-	7.87	3.04	7.25	-	-
MgO	11.90	18.89	11.22	9.00	8.21	7.50
MnO	0.20	0.15	0.05	0.18	0.22	-
CaO	10.80	5.94	11.62	10.50	10.30	15.90
Na_2O	2.90	4.92	2.30	2.75	0.39	0.60
K_2O	1.30	0.57	0.46	0.80	0.08	-
SO_3	-	0.11	0.10	-	-	-
SrO	-	-	-	-	-	-
P_2O_5	0.60	-	-	0.80	0.05	-
Total	98.40	99.56	100	98.78	99.58	100

Table 3. Summary of the EDX spot collection count for each lunar regolith simulant for EAC-1A [72] *and Mineralogy Weight percent, as mixed for LMS-1 and LHS-1* [68].

	EAC-1A	**LMS-1**	**LHS-1**
		(wt%)	*(wt%)*
Plagioclase	17	32.8	74.4
Glass	-	24.5	24.2
Basalt	-	19.8	0.5
Ilmenite	-	11.1	0.4
Pyroxene	22	7.5	0.3
Olivine	14	4.3	0.2
Iron Oxide	13	-	-
Other	8	-	-
Total	74	100	100

3.2. Particle size distribution

Lunar regolith was found to have log-normal size distribution with mean diameters typically between 45 µm and 100 µm, although particles can be as small as 10 nm [73][74]. Fig. 5 shows particle size data on the three selected as received simulants.

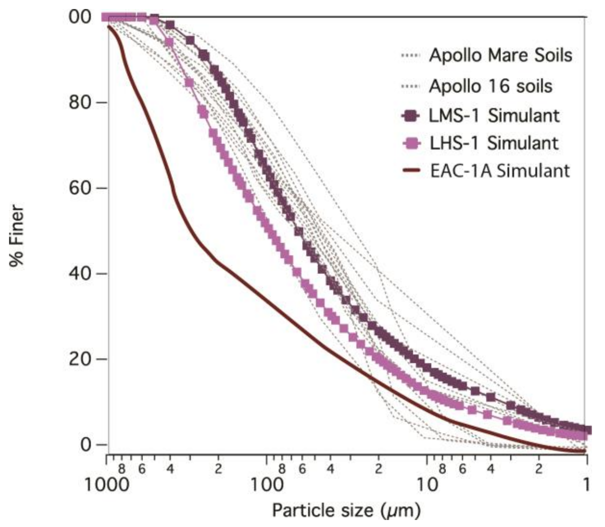

Figure 5. Average particle size distribution for EAC-1A [75]*, LMS-1, and LHS-1. Apollo data has been adjusted to remove the >1 mm fraction* [68]*.*

The particle size range for EAC-1A is 0.02 - 2000 µm [75]. The particle size range for LHS-1 and LMS-1 simulants is <1 µm – 1000 µm. The Mean Particle Size is 94 µm for LHS-1 and 63 µm for LMS-1 (Fig. 5). In all three simulants there is a significant fraction of large grains (>1mm), which is problematic for additive manufacturing. Thus, for the selected technique in this study, first a sieving or crushing process will be required to remove the greater fraction. Once processed in this way, further investigation into the size distribution of the simulant will be employed to assess potential sintering characteristics.

3.3. Particle shape

The particle shape has great influence over the flow and packing behaviour of powders, which affects in turn the properties of the consolidated material. Lunar particles are irregular in shape and have high cohesion in comparison to terrestrial materials, due to the environmental factors of the lunar surface; as a result, lunar regolith is highly abrasive (Fig. 6) [76]. This abrasive property is difficult to simulate using Earth material, which should be taken into account during this feasibility study. From initial observations, LMS-1 and LHS-1 particles exhibit larger particle elongation and lower circularity than EAC-1A. Quantitative shape analysis using image analysis software will be required to fully understand the expected behaviour of the powder under processing.

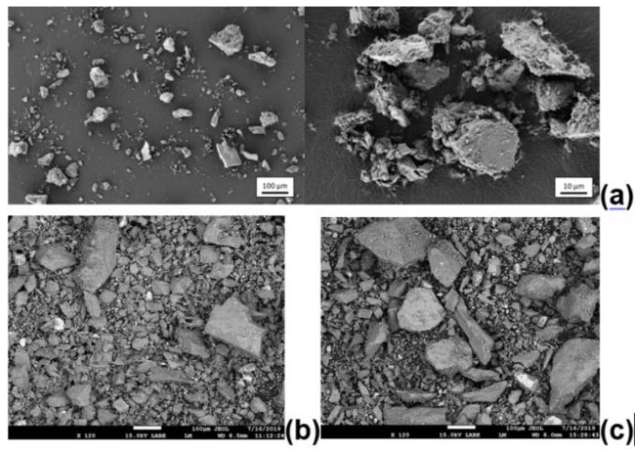

Figure 6. SEM images for EAC-1A (a) [75]*, LHS-1(b), and LMS-1 (c)* [68]*.*

3.4. Bulk density

Most AM techniques involve the loose deposition of one material layer over another one. For this reason, *poured bulk density* was measured instead of *tapped density*. Poured density is useful in this study to determine the quantity of material required for the manufacturing process. Measurements on lunar soil samples, namely Apollo 14 and Apollo 15, have revealed bulk densities that vary from a minimum 0.87 g/cm^2 to a maximum 1.89 g/cm^2**.** The reason for this variation is related to specific gravity, re-entrant intra-granular voids, particle shape, particle size distribution, and surface texture [77].

Poured bulk density was measured for simulants EAC-1A, LMS-1 and LHS-1 in accordance with ASTM D7481-18 (Standard Test Methods for Determining Loose and Tapped Bulk Densities of Powders using a Graduated Cylinder) [78]. For each simulant, three 100 g powder samples were poured into a 100 mL graduated cylinder and levelled; Eq. 1 was used to calculate density ρ, where m is the mass of the sample (g), and V is the untapped volume occupied by the simulant (cm^3):

$$\rho = \frac{m}{V} \tag{1}$$

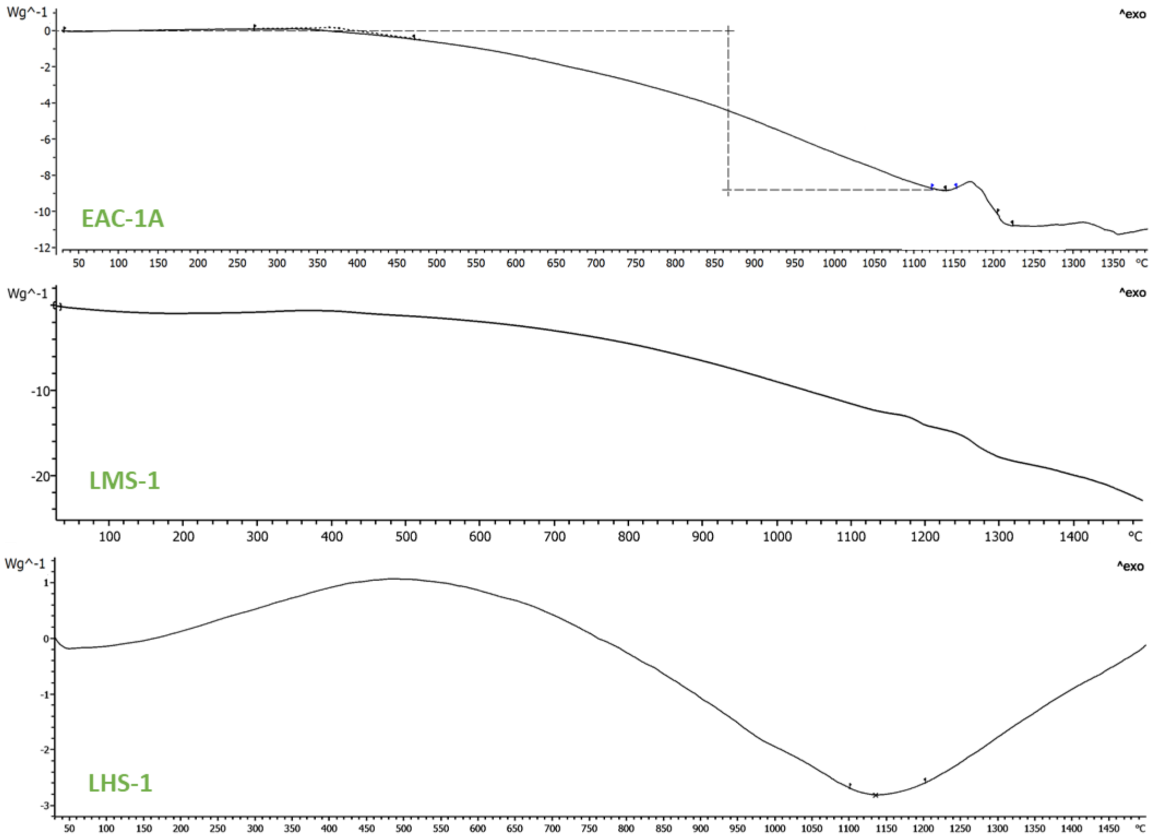

Figure 7. DSC traces for EAC-1A (above), LMS-1 (center) and LHS-1 (below)

Three measurements were carried per sample, with results derived from the mean. In comparison with lunar samples, the simulants exhibit similar poured bulk densities of 1.50g/cm^3 for EAC-1A, 1.60g/cm^3 for LMS-1 and 1.61g/cm^3 for LHS-1.

3.5. Thermal analysis

Regolith is a multi-constituent aggregate consisting of several mineralogical components. It is useful to understand the thermal behaviour of these components in order to estimate appropriate processing temperatures. A technique coupling Thermogravimetric Analysis (TGA) with Differential Scanning Calorimetry (DSC) was used to identify thermal transition temperatures for each sample. Using a calibrated Mettler Toledo TGA/DSC 3+ instrument, all three simulants were heated from room temperature to above 1400°C at a rate of 10K/min for EAC-1A and LHS-1 samples and a rate of 50K/min for LMS-1 sample. The tests were performed under an argon atmosphere with a constant gas flow of 70 ml/min. Additionally, a blank curve was obtained under the same conditions as each sample, in order to account for buoyancy and the effects of the instrument. Fig. 7 shows DSC curves normalized to sample temperature for EAC-1A, LMS-1 and LHS-1 simulants. All three samples exhibit transformations in the 1100 - 1350°C region. This is consistent with the melting of basalt, ilmenite and glass [59][79] which are present in the given simulants in varying quantity, see Tab.3. The exhibited thermal behaviour may also be attributed to the melting or partial-melting of plagioclase. In lunar regolith the plagioclase is assumed to be of the high-Ca type anorthite which has a melting temperature around 1550°C. However the presence of Na_2O oxide in the bulk chemistry suggests plagioclase may have undergone partial melting, as the plagioclase solidus temperature is known to decrease with increasing sodium content [80][81]. Thus, at sintering temperatures in the range 1250 - 1350°C or above, some regolith melting should be expected.

From the TGA results, the following values of mass loss were recorded, in the temperature range [30, 1350]°C. When heated above 1350°C, mass losses of 0.97% for LMS-1, 1.07% for LHS-1 and 2.75% for EAC-1A were observed. These losses can be attributed to loss of water and the release of other volatiles at higher temperatures. To emulate lunar surface conditions most effectively, simulants should be furnace dried to remove volatiles before processing.

4. DISCUSSION and CONCLUSION

Powder characterization was performed on three lunar simulants to determine the feasibility of additively manufacturing and FGM. Metal oxides have been identified in the lunar regolith, which implies that in-situ extraction of metal is plausible. The compatibility of a gradient from metal to lunar simulant should be further investigated. Powder characterization of regolith simulant provides insight on how to fabricate the gradient. Based on this study, the following consolidation techniques were selected: additive manufacturing via DPL and conventional bulk consolidation via SPS. These techniques are suitable for both ceramic and metal powders and thus FGM. It was also found that prior to consolidation, the simulant powder requires preparation, particularly sieving and crushing due to the large particle size. The expected manufacturing challenges will be regarding mismatch in coefficient of thermal expansion and material composition behaviour during sintering. Optionally, crack prevention and delamination can be investigated to prevent parts failure and poor bonding between substrate materials.

To conclude, FGMs have a great potential for in-situ manufacturing on the lunar surface. It should be noted that while this study is focused on the space habitats, other aerospace components can also be considered. Future work will focus on further characterisation of lunar simulant and development of a thermal model of the FGM powder consolidation, to employ the selected bulk consolidation techniques for production of FGM material.

REFERENCES

[1] H. Benaroya, *Building Habitats on the Moon: Engineering Approaches to Lunar Settlements*. Springer, 2018.

[2] P. Eckart, *The lunar base handbook: an introduction to lunar base design, development, and operations*. McGraw-Hill, 1999.

[3] H. Benaroya, *Lunar settlements*. CRC Press, 2010.

[4] W. Grandl, “Lunar Base 2015 Stage 1,” *Acta Astronaut.*, vol. 60, no. 4–7, pp. 554–560, 2007.

[5] K. J. Kennedy, “The vernacular of space architecture,” *AIAA Sp. Archit. Symp.*, no. October, pp. 1–15, 2002.

[6] P. Gruber, S. Häuplik, B. Imhof, K. Özdemir, R. Waclavicek, and M. A. Perino, “Deployable structures for a human lunar base,” *Acta Astronaut.*, vol. 61, no. 1–6, pp. 484–495, 2007.

[7] A. S. Howe and B. Sherwood, *Out of this world: The new field of space architecture*. American Institute of Aeronautics and Astronautics, 2009.

[8] M. Z. Naser and A. I. Chehab, “Materials and design concepts for space-resilient structures,” *Prog. Aerosp. Sci.*, vol. 98, no. March, pp. 74–90, 2018.

[9] N. Labeaga-Martínez, M. Sanjurjo-Rivo, J. Díaz-Álvarez, and J. Martínez-Frías, “Additive manufacturing for a Moon village,” *Procedia Manuf.*, vol. 13, pp. 794–801, 2017.

[10] T. Kim, M. Roman, and R. Mueller, “NASA ’ s Centennial Challenge for 3D-Printed Habitat : Phase II Outcomes and Phase III Competition Overview,” 2018.

[11] W. Grandl, “Design and Construction of a Modular Lunar Base,” *38th COSPAR Sci. Assem. Held 18-15 July 2010, Bremen, Ger. p.2.*, 2010.

[12] G. Sanders *et al.*, “Results from the NASA Capability Roadmap Team for In-Situ Resource Utilization (ISRU),” *ILEWG Conf. Explor. Util. Moon (7th), Sept 18-23*, pp. 1–17, 2005.

[13] Y. li Gao, C. shan Wang, M. Yao, and H. bin Liu, “The resistance to wear and corrosion of laser-cladding Al2O3ceramic coating on Mg alloy,” *Appl. Surf. Sci.*, vol. 253, no. 12, pp. 5306–5311, 2007.

[14] X. Zhang, Y. Chen, and J. Hu, “Recent advances in the development of aerospace materials,” *Prog. Aerosp. Sci.*, vol. 97, no. August 2017, pp. 35–60, 2018.

[15] M. B. Bever and P. E. Duwez, “Gradients in composite materials,” *Mater. Sci. Eng.*, vol. 10, no. C, pp. 1–8, 1972.

[16] B. H. Kim and Y. H. Na, “Fabrication of fiber-reinforced porous ceramics of Al2O3-mullite and SiC-mullite systems,” *Ceram. Int.*, vol. 21, no. 6, pp. 381–384, 1995.

[17] S. Suresh and A. Mortensen, “Functionally graded metals and metal-ceramic composites: Part 2 Thermomechanical behaviour,” *Int. Mater. Rev.*, vol. 42, no. 3, pp. 85–116, 1997.

[18] X. Wang *et al.*, “Thermal protection system integrating graded insulation materials and multilayer ceramic matrix composite cellular sandwich panels,” *Compos. Struct.*, vol. 209, pp. 523–534, 2019.

[19] M. Naebe and K. Shirvanimoghaddam, “Functionally graded materials: A review of fabrication and properties,” *Appl. Mater. Today*, vol. 5, pp. 223–245, 2016.

[20] D. C. Hofmann *et al.*, “Compositionally graded metals: A new frontier of additive manufacturing,” *J. Mater. Res.*, vol. 29, no. 17, pp. 1899–1910, 2014.

[21] A. Kawasaki and R. Watanabe, “Concept and P/M fabrication of functionally gradient materials,” *Ceram. Int.*, vol. 23, no. 1, pp. 73–83, 1997.

[22] D. Mahmoud and M. Elbestawi, “Lattice Structures and Functionally Graded Materials Applications in Additive Manufacturing of Orthopedic Implants: A Review,” *J. Manuf. Mater. Process.*, vol. 1, no. 2, p. 13, 2017.

[23] N. Oxman, S. Keating, and E. Tsai, “Functionally graded rapid prototyping,” *Innov. Dev. Virtual Phys. Prototyp.*, pp. 483–489, 2012.

[24] M. Srivastava, S. Rathee, S. Maheshwari, and T. K. Kundra, “Design and processing of functionally graded material: review and current status of research,” in *3D Printing and additive manufacturing technologies*, Springer, 2019, pp. 243–255.

[25] V. A. Popovich, E. V Borisov, V. Heurtebise, T. Riemslag, A. A. Popovich, and V. S. Sufiiarov, “Creep and thermomechanical fatigue of functionally graded inconel 718 produced by additive manufacturing,” in *TMS 2018 - 147th Annual Meeting and Exhibition*, 2018, pp. 85–97.

[26] V. K. Balla, P. P. Bandyopadhyay, S. Bose, and A. Bandyopadhyay, “Compositionally graded yttria-stabilized zirconia coating on stainless steel using laser engineered net shaping (LENS™),” *Scr. Mater.*, vol. 57, no. 9, pp. 861–864, 2007.

[27] J. Sun, Z. Li, X. Ni, F. Gong, J. Zhao, and G. Hou, “Design, fabrication and mechanical properties of multidimensional graded ceramic tool materials,” *Ceram. Int.*, vol. 44, no. 3, pp. 2941–2951, 2017.

[28] H. L. Hou, X. P. Ren, Y. L. Zhang, Q. Jin, and H. T. Qu, “*In Situ* Synthesis and Structural Design of Ti/TiC Functionally Graded Materials,” *Mater. Sci. Forum*, vol. 913, pp. 515–521, 2018.

[29] F. F. Kamaruzaman, D. M. Nuruzzaman, N. M. Ismail, Z. Hamedon, A. K. M. A. Iqbal, and A. Azhari, “Microstructure and properties of aluminium-aluminium oxide graded composite materials,” *IOP Conf. Ser. Mater. Sci. Eng.*, vol. 319, no. 1, pp. 0–6, 2018.

[30] A. Katz-demyanetz, V. V. P. Jr, A. Kovalevsky, and D. Safranchik, “Powder-bed additive manufacturing for aerospace application : Techniques , metallic and metal / ceramic composite materials and trends,” vol. 5, 2019.

[31] S. W. Maseko, A. P. I. Popoola, and O. S. I. Fayomi, “Characterization of ceramic reinforced titanium matrix composites fabricated by spark plasma sintering for anti-ballistic applications,” *Def. Technol.*, vol. 14, no. 5, pp. 408–411, 2018.

[32] T. A. Guisard Restivo *et al.*, “Micrograded ceramic-metal composites,” *J. Eur. Ceram. Soc.*, 2019.

[33] M. Toozandehjani, “Conventional and Advanced Composites in Aerospace Industry: Technologies Revisited,” *Am. J. Aerosp. Eng.*, vol. 5, no. 1, p. 9, 2019.

[34] B. Zhu and Y. Cai, “Particle Size-Dependent Responses of Metal–Ceramic Functionally Graded Plates Under Low-Velocity Impact,” *Int. J. Appl. Mech.*, vol. 10, no. 05, p. 1850056, 2018.

[35] G. H. Heiken, D. T. Vaniman, and B. M. French, “Lunar sourcebook-A user’s guide to the moon,” *Res. Support. by NASA,. Cambridge, England, Cambridge Univ. Press. 1991, 753 p. No Individ. items are Abstr. this Vol.*, 1991.

[36] J. J. Papike, S. B. Simon, and J. C. Laul, “The lunar regolith: Chemistry, mineralogy, and petrology,” *Rev. Geophys.*, vol. 20, no. 4, pp. 761–826, 1982.

[37] J. Edmunson and D. L. Rickman, “A Survey of Geologic Resources,” in *Moon*, Springer, 2012, pp. 1–21.

[38] G. A. Landis, “Materials refining on the Moon,” *Acta Astronaut.*, vol. 60, no. 10–11, pp. 906–915, 2007.

[39] D. J. Lawrence, “Volatiles on the Lunar Surface and Subsurface,” 2015.

[40] M. F. McKay, D. S. McKay, and M. B. Duke,

"Space resources. Volume 2: Energy, power, and transport," 1992.

[41] B. A. Lomax, M. Conti, N. Khan, N. S. Bennett, A. Y. Ganin, and M. D. Symes, "Proving the viability of an electrochemical process for the simultaneous extraction of oxygen and production of metal alloys from lunar regolith," *Planet. Space Sci.*, p. 104748, 2019.

[42] Y. Hu and W. Cong, "A review on laser deposition-additive manufacturing of ceramics and ceramic reinforced metal matrix composites," *Ceram. Int.*, vol. 44, no. 17, pp. 20599–20612, 2018.

[43] M. Ivosevic, R. Knight, S. R. Kalidindi, G. R. Palmese, and J. K. Sutter, "Solid particle erosion resistance of thermally sprayed functionally graded coatings for polymer matrix composites," *Surf. Coatings Technol.*, vol. 200, no. 16–17, pp. 5145–5151, 2006.

[44] G. E. Knoppers, J. W. Gunnink, J. Van Den Hout, and W. P. Van Vliet, "The reality of functionally graded material products," *Proc. Solid Free. Fabr. Symp.*, pp. 38–43, 2004.

[45] Q. Shu-heng, Y. Jun-li, C. Xue-min, Z. Lin, and L. Le-ping, "Preparation of phosphoric acid-based porous geopolymers," *Appl. Clay Sci.*, vol. 50, no. 4, pp. 600–603, 2010.

[46] H. A. Toutanji, S. Evans, and R. N. Grugel, "Performance of lunar sulfur concrete in lunar environments," *Constr. Build. Mater.*, vol. 29, pp. 444–448, 2012.

[47] C. Buchner, R. H. Pawelke, T. Schlauf, A. Reissner, and A. Makaya, "A new planetary structure fabrication process using phosphoric acid," *Acta Astronaut.*, vol. 143, no. October 2017, pp. 272–284, 2018.

[48] R. Dou *et al.*, "Sintering of lunar regolith structures fabricated via digital light processing," *Ceram. Int.*, 2019.

[49] X. Zhang *et al.*, "Microstructure evolution during spark plasma sintering of FJS-1 lunar soil simulant," *J. Am. Ceram. Soc.*, no. September, pp. 1–13, 2019.

[50] S. Maleksaeedi, H. Eng, F. E. Wiria, T. M. H. Ha, and Z. He, "Property enhancement of 3D-printed alumina ceramics using vacuum infiltration," *J. Mater. Process. Technol.*, vol. 214, no. 7, pp. 1301–1306, 2014.

[51] A. R. J. Meurisse, A. Cowley, S. Cristoforetti, A. Makaya, L. Pambaguian, and M. Sperl, "Solar 3D printing of lunar regolith," *Acta Astronaut.*, no. February, pp. 0–1, 2018.

[52] S. Rana and R. Fangueiro, *16 - Conclusions and future trends*. Elsevier Ltd, 2016.

[53] D. C. Hofmann *et al.*, "Developing gradient metal alloys through radial deposition additive manufacturing," *Sci. Rep.*, vol. 4, 2014.

[54] Y. Zhang and A. Bandyopadhyay, "Direct fabrication of compositionally graded Ti-Al2O3multi-material structures using Laser Engineered Net Shaping," *Addit. Manuf.*, vol. 21, pp. 104–111, 2018.

[55] M. Liu *et al.*, "Digital light processing of lunar regolith structures with high mechanical properties," *Ceram. Int.*, vol. 45, no. 5, pp. 5829–5836, 2019.

[56] R. N. Grugel and H. Toutanji, "Sulfur 'concrete' for lunar applications - Sublimation concerns," *Adv. Sp. Res.*, vol. 41, no. 1, pp. 103–112, 2008.

[57] M. Fateri and A. Gebhardt, "Process parameters development of selective Laser Melting of lunar regolith for on-site manufacturing applications," *Int. J. Appl. Ceram. Technol.*, vol. 12, no. 1, pp. 46–52, 2015.

[58] A. Goulas, R. A. Harris, and R. J. Friel, "Additive manufacturing of physical assets by using ceramic multicomponent extra-terrestrial materials," *Addit. Manuf.*, vol. 10, pp. 36–42, 2016.

[59] A. Meurisse, A. Makaya, C. Willsch, and M. Sperl, "Solar 3D printing of lunar regolith," *Acta Astronaut.*, vol. 152, no. June, pp. 800–810, 2018.

[60] M. Fateri *et al.*, "Solar Sintering for Lunar Additive Manufacturing," *J. Aerosp. Eng.*, vol. 32, no. 6, pp. 1–10, 2019.

[61] G. Cesaretti, E. Dini, X. De Kestelier, V. Colla, and L. Pambaguian, "Building components for an outpost on the Lunar soil by means of a novel 3D printing technology," *Acta Astronaut.*, vol. 93, pp. 430–450, 2014.

[62] C. J. Bae, A. Ramachandran, K. Chung, and S. Park, "Ceramic stereolithography: Additive manufacturing for 3D complex ceramic structures," *J. Korean Ceram. Soc.*, vol. 54, no. 6, pp. 470–477, 2017.

[63] "SLA vs. DLP: Compare Resin 3D Printers (2020 Guide) | Formlabs." .

[64] P. C. Editor, *Spark Plasma Sintering of Materials*. 2019.

[65] L. Song *et al.*, "Vacuum sintered lunar regolith simulant: Pore-forming and thermal conductivity," *Ceram. Int.*, vol. 45, no. 3, pp. 3627–3633, 2019.

[66] E. J. Faierson, K. V. Logan, B. K. Stewart, and M. P. Hunt, "Demonstration of concept for fabrication of lunar physical assets utilizing lunar regolith simulant and a geothermite reaction,"

Acta Astronaut., vol. 67, no. 1–2, pp. 38–45, 2010.

[67] M. A. Hobosyan and K. S. Martirosyan, “SINTERING OF REGOLITH BY ACTIVATED THERMITES: A NOVEL APPROACH FOR LUNAR IN SITU RESOURCE UTILIZATION.”

[68] K. Cannon, *Planetary simulant database, https://sciences.ucf.edu/class/exolithlab*. 2019.

[69] V. E. Nash, A. Cowley, M. Fateri, S. Coene, S. Siarov, and S. Cristoforetti, “Human Exploration Initiatives at EAC: Spaceship EAC and the Development of Large-Volume Lunar Regolith Simulant for LUNA,” in *European Planetary Science Congress*, 2017, vol. 11.

[70] L. Sibille, P. Carpenter, R. Schlagheck, and R. A. French, “Lunar regolith simulant materials: recommendations for standardization, production, and usage,” 2006.

[71] J. Schleppi, J. Gibbons, A. Groetsch, J. Buckman, A. Cowley, and N. Bennett, “Manufacture of glass and mirrors from lunar regolith simulant,” *J. Mater. Sci.*, vol. 54, no. 5, pp. 3726–3747, 2019.

[72] B. A. Lomax, “Characterisation and evaluation of lunar regolith simulants for use in in-situ resource utilisation research,” *Submitt. degree Master Sci. Inst. Mech. Process Energy Eng. Heriot-Watt Univ.*, p. 54, 2018.

[73] P. S. Greenberg, D.-R. Chen, and S. A. Smith, “Aerosol measurements of the fine and ultrafine particle content of lunar regolith,” 2007.

[74] Y. Liu, D. W. Schnare, B. C. Eimer, and L. A. Taylor, “Dry separation of respirable lunar dust: providing samples for the lunar airborne dust toxicity advisory group,” *Planet. Space Sci.*, vol. 56, no. 11, pp. 1517–1523, 2008.

[75] P. Nieke, J. Kita, M. Häming, and R. Moos, “Manufacturing Dense Thick Films of Lunar Regolith Simulant EAC-1 at Room Temperature,” *Materials (Basel).*, vol. 12, no. 3, p. 487, 2019.

[76] L. A. Taylor and Y. Liu, “Important considerations for lunar soil simulants,” in *Earth and Space 2010: Engineering, Science, Construction, and Operations in Challenging Environments*, 2010, pp. 106–118.

[77] I. I. I. Carrier W.~D., J. ~K. Mitchell, and A. Mahmood, “The relative density of lunar soil,” *Lunar Planet. Sci. Conf. Proc.*, vol. 4, p. 2403, Jan. 1973.

[78] D7481-18ASTM, *Standard test methods for determining loose and tapped bulk densities of powders using a graduated cylinder. ASTM International*. 2018.

[79] X. Chen, Y. Zhang, D. Hui, M. Chen, and Z. Wu, “Study of melting properties of basalt based on their mineral components,” *Compos. Part B Eng.*, vol. 116, pp. 53–60, 2017.

[80] A. Tsuchiyama and E. Takahashi, “Melting kinetics of a plagioclase feldspar,” *Contrib. to Mineral. Petrol.*, vol. 84, no. 4, pp. 345–354, 1983.

[81] V. Badescu, Ed., *Moon*. Berlin, Heidelberg: Springer Berlin Heidelberg, 2012.